



**HAL**  
open science

# Exact solutions for signal propagation along an excitable transmission line

Arnaud Tonnelier

► **To cite this version:**

Arnaud Tonnelier. Exact solutions for signal propagation along an excitable transmission line. Physical Review E , 2024, 109, pp.014219. 10.1103/PhysRevE.109.014219 . hal-04349848

**HAL Id: hal-04349848**

**<https://hal.science/hal-04349848>**

Submitted on 18 Dec 2023

**HAL** is a multi-disciplinary open access archive for the deposit and dissemination of scientific research documents, whether they are published or not. The documents may come from teaching and research institutions in France or abroad, or from public or private research centers.

L'archive ouverte pluridisciplinaire **HAL**, est destinée au dépôt et à la diffusion de documents scientifiques de niveau recherche, publiés ou non, émanant des établissements d'enseignement et de recherche français ou étrangers, des laboratoires publics ou privés.



Distributed under a Creative Commons Attribution 4.0 International License

# Exact solutions for signal propagation along an excitable transmission line.

Arnaud Tonnelier

*Univ. Grenoble Alpes, Inria, CNRS, Grenoble INP, LJK, 38000 Grenoble, France.\**

(Dated: December 7, 2023)

A simple transmission line composed of pulse-coupled units is presented. The model captures the basic properties of excitable media with, in particular, the robust transmission of information via traveling wave solutions. For rectified linear units with a cut-off threshold, the model is exactly solvable and analytical results on propagation are presented. The ability to convey a non-trivial message is studied in detail.

## I. INTRODUCTION

Nonlinear media have been largely used for their information-processing capabilities, and, among them, excitable media have become a paradigm for performing natural or unconventional computing [11, 17]. A bit of information is physically represented by a pulse excitation and a group of pulses delivers a message [2]. The non-equilibrium properties of the medium can be used to generate nontrivial messages and, in spatially extended system, the question of information transmission is closely related to the existence of traveling wave solutions. The ability of discrete excitable media to support nonlinear waves is well known in biology [23] but has also been observed in geochemical systems [15], chemical reaction kinetics [37], and in engineered systems [24, 25], to mention few of them. Traveling waves are directly involved in information processing as for instance in visual perception [38] and more broadly in the functions performed by the nervous system [1]. The temporal structure of the wave plays an important role in the neural processing of sensory stimuli. In particular, the synaptic plasticity, involved in learning and memory, crucially depends on the precise timing of pulses [22].

A fundamental issue in the study of collective dynamics is to unravel the complex relation between interactions and dynamics, specially for functionally meaningful trajectories, i.e. having non-trivial spatio-temporal profiles [20, 31]. In most natural systems, the precise network structure is unknown and information about the connectivity is obtained indirectly from activity measurement [26]. The absence or presence of a connection, or the hierarchical structure of the network, can be inferred from the dynamical response properties [3, 30]. In this context, we raise the following question: given a network structure, say regular lattice, all-to-all connectivity, or random network, is it possible to derive information on connectivity strength from signal propagation? It is well documented that a weak connectivity does not allow for propagation, a phenomenon known as propagation failure. The strength of each connection shapes the dynam-

ics of propagation but finding the precise relation between traveling waves and network connectivity remains a challenging problem.

Detailed models provide a comprehensive description of excitable networks but they are rarely integrable and their study reveals to be very difficult beyond numerical simulations. Valuable insights into the dynamics of nonlinear waves in excitable media have been obtained using simplified models [4, 7]. Analytical results based on explicit solutions have proven useful in understanding propagation phenomena in nonlinear transmission lines [32]. In this paper we introduce a simple threshold model that captures the basic properties of excitable media with, in particular, the existence of different propagating patterns. The complete solvability of the model allows an in-depth analysis of simple waves where units along the network are sequentially activated [34] and of complex patterns having a non-trivial spatio-temporal periodicity [33].

The plan of the paper is the following. In the next section, the generic formulation of the excitable transmission line is presented. In section III preliminary results on existence and stability of traveling signals are obtained. A fully solvable model is proposed and studied in section IV where analytical expressions are derived for both the signal shape and the signal velocity.

## II. THE EXCITABLE TRANSMISSION LINE

We study the signals generated and propagated by one-dimensional networks where each node is described by a time-dependent state variable, noted  $s_i(t)$ , where  $i \in \mathcal{Z}$  is the index of the node in the network and  $t > 0$  is the time. The mechanisms of emission and transmission along the network are as follow. A node may interact with the others in the network if its activation threshold is reached. The  $i^{th}$  node is said to be activated at time  $t_i$  when  $s_i(t_i) \geq 1$ , where we set without loss of generality the threshold to unity. The threshold-crossing time  $t_i$  is called indifferently the activation time, the firing time or the excitation time. The firing time is transmitted so that the dynamics of the node at location  $i$  is described

---

\* arnaud.tonnelier@inria.fr

by

$$s_i(t) = \sum_j w_{ij} e(t - t_j), \quad (1)$$

where  $w_{ij}$  is the strength of the connection from  $j$  to  $i$  and  $e(t)$  is a pulse-shape coupling function that is initiated by the arrival of a firing time (at time  $t_j$ ). Its analytical expression will be specified latter. We assume that the network is homogeneous, we have  $w_{ij} = w(i-j)$ , feedforward, that is  $w_{i,j} = 0$  for  $j \geq i$ , and excitatory, i.e.  $w_{ij} \geq 0$ . We note  $w_j = w_{i,i-j}$  and  $n$  the maximum connection length, i.e.  $w_j = 0$ , for  $j > n$ . After the transmission of the firing time, the node remains quiescent, i.e. a strong refractory is assumed (the node jumps back instantly to 0). The single-activation approximation is relevant in rapid information processing tasks as, for instance, in fast image recognition where each processing unit, the neuron, can emit only one action potential [29]. This situation also occurs when the recovery operates on a time scale significantly greater than the activation as in forest fires or epidemic spread. The single-spike solution is also used to facilitate the mathematical treatment of models [35].

The excitable transmission line described by (1) shares similarities with pulse-coupled neural networks, named PCNN, that have been primarily introduced to describe the dynamics of the visual cortex [6]. It is also a particular instantiation of the spike response model [10] where the emission times  $t_i$  are the spike timings and the elementary signal  $e(t)$  is the excitatory postsynaptic potential. The model can be derived from an approximation of differential models of biological neural networks [33]. It allows a continuous time integration of incoming signals and therefore differs from cellular automata that are synchronously updated [39].

Determining exact solutions of the excitable system (1) relies on finding a closed-form expression for the activation times  $t_i$ . We are interested in the propagation along the transmission line that is, in the trivial case, associated with the existence of an increasing sequence ( $t_i$ ) where the successive activation times of the nodes along the network increase linearly, i.e. we have  $t_{i+1} - t_i = 1/c$  where  $c$  is the transmission speed. However, more complex relation between successive firing times can exist and we are set out to construct traveling signals with a non-trivial spatiotemporal periodicity. This leads to solutions that are less understood and that correspond to an intriguing behavior closely related to the lurching waves observed in continuous excitable networks [12, 13, 27] and to multichromatic travelling waves recently found in lattice Nagumo equations [18, 19]. The periodicity of these traveling patterns does not come from the periodic structure of the underlying medium, as for instance in diatomic chains [16] or in synfire-chains [2], but arises as a natural property of spatially homogeneous systems. This also differs from the propagation of spatio-temporal patterns generated by the successive excitation of individual elements as in burst propagation [28]; a solution tied to

intrinsic nodes properties rather than connectivity.

### III. TRAVELING SIGNALS

We consider the transmission of firing sequences described by a velocity,  $c$ , and a sequence of time-intervals, noted  $(s_k)$ , such that the activation times of the nodes along the lattice are given by  $t_{pi+k} = (pi+k)/c + s_k$  which characterizes the  $i$ th repetition of a sequence of length  $p$ , i.e. involving  $p$  successive nodes. We have  $k \in 0, \dots, p-1$  that denotes the label of the nodes in the replaying sequence. We fix the origin of the sequence at  $k=0$  and we set  $s_0=0$ . The case  $s_k=0$  corresponds to the propagation of simple signals where the successive activation times have a constant time shift of  $1/c$ . The sequence  $(s_k)$  measures how the propagating signal deviates from a simple signal and we refer this solution as a composite signal to suggest that the propagation can be seen as the combination of simple signals where distinct nodes can have distinct profiles.

A fundamental question is how the sequence  $(s_k)$  and the velocity  $c$  are related to the network connectivity, i.e. the weights  $(w_j)$ ? In this paper, we focus on third nearest-neighbor interactions, i.e. we set  $n=3$ , that corresponds to the simplest connectivity that allows the propagation of composite signals of length  $p=2$ . The existence of a traveling packet of two firing times is determined by the two unknowns,  $c$  and  $s$ , such that

$$t_i = \begin{cases} \frac{i}{c}, & \text{if } i \text{ is odd,} \\ \frac{i}{c} + s, & \text{if } i \text{ is even,} \end{cases} \quad (2)$$

The transmission line conveys two time intervals: the natural one associated with the velocity and an additional information, coded by  $s$ . The characteristic time  $s$  is an intrinsic property of the transmission line and not a free parameter. The case  $s=0$  corresponds to a simple signal and the case  $s=1/c$  is related to the propagation of a synchronous pair of firing times. Traveling signals associated with the activation times (2) have two distinct profiles, noted  $S_1$  and  $S_2$ , such that

$$s_i(t) = \begin{cases} S_1(i-ct), & \text{if } i \text{ is odd,} \\ S_2(i-ct), & \text{if } i \text{ is even,} \end{cases}$$

that are given by

$$\begin{cases} S_1(\xi) = w_1 e(\xi + \frac{1}{c} - s) + w_2 e(\xi + \frac{2}{c}) + w_3 e(\xi + \frac{3}{c} - s), \\ S_2(\xi) = w_1 e(\xi + \frac{1}{c} + s) + w_2 e(\xi + \frac{2}{c}) + w_3 e(\xi + \frac{3}{c} + s), \end{cases} \quad (3)$$

where  $\xi$  is the traveling wave coordinate. Threshold condition for the traveling wave solutions gives

$$f(1/c, s) = 0, \text{ and } f(1/c, -s) = 0, \quad (4)$$

where  $f(x, y) = w_1 e(x-y) + w_2 e(2x) + w_3 e(3x-y) - 1$ . A solution of (4) is associated with a traveling signal if the admissibility conditions

$$S_i(\xi) < 1 \quad \text{for } \xi < 0, \quad i = 1, 2 \quad (5)$$

are fulfilled. Otherwise the solution is said to be non-admissible. Inequalities (5) ensure that the threshold is not reached before the origin and can be interpreted as causality conditions.

Stability is a key property for the robust propagation of signals along the network. We consider a small perturbation of the emitting times such that  $\tilde{t}_i = t_i + u_i$  where  $|u_i| \ll 1$ . We inject this ansatz into (1) and we look for a solution of the form  $u_{2i} = \lambda_1^i \lambda_2^i$  and  $u_{2i+1} = \lambda_1 u_{2i}$  in the linearized system. Asymptotic stability of the traveling sequence (2) holds when  $|\lambda_1 \lambda_2| \leq 1$  where  $\lambda_1$  and  $\lambda_2$  are the roots of the multivariate polynomials

$$\begin{aligned} (a + b + c)x^2y - axy - bx - c &= 0, \\ (\bar{a} + \bar{b} + \bar{c})xy^2 - \bar{a}xy - \bar{b}y - \bar{c} &= 0, \end{aligned} \quad (6)$$

where the coefficients are given by  $a = w_1 e'(1/c + s)$ ,  $b = w_2 e'(2/c)$ ,  $c = w_3 e'(3/c + s)$ , with  $e'$  the derivative of the coupling function  $e$ . Coefficients  $(\bar{a}, \bar{b}, \bar{c})$  are directly obtained from  $(a, b, c)$  replacing  $s$  by  $-s$  in the corresponding expression. The trivial solution  $\lambda_1 = \lambda_2 = 1$  is related to the translational invariance of traveling wave solutions.

Traveling signals are classified into two distinct types. The case  $s = 0$  corresponds to simple signals that are characterized by a constant interspike interval between two consecutive nodes. Within this class, we distinguish between three different solutions reported as 3-signal, 2-signal and 1-signal that are classified according to the location of the time events  $t_i = 1/c$ ,  $i = 1, 2, 3$ , with respect to the time-to-peak of the pulse-shape function  $e$ . If the three events fall into the increasing phase of  $e$ , the traveling signal belongs to the 3-signals class. The 1-signal is obtained if  $1/c$  is the only time less than the time-to-peak. The intermediate solution corresponds to a 2-signal. The 3-signals are fast wave where each firing time of neighboring nodes contributes to the threshold crossing so that 3-signals are strictly monotone whereas for 2-signals and 1-signals the effect of the received-first and received-second firing time, respectively, has vanished or is in a decaying phase at the threshold crossing. When  $s > 0$  the solution corresponds to a composite signal and we distinguish between the case  $s < 1/c$  where the firing sequence is strictly increasing and  $s > 1/c$  where the sequence is non monotonic.

#### IV. AN EXACTLY SOLVABLE MODEL

We consider a coupling function  $e$  given by the cut-off ramp function

$$e(t) = t, \quad \text{for } 0 \leq t \leq 1, \quad (7)$$

and 0 otherwise, that can be rewritten as  $e(t) = t\chi_{[0,1]}(t)$  where  $\chi$  is the indicator function. The ramp function, or rectified function, is omnipresent in digital signal processing and is frequently used to describe a progressive

excitation. In our model we add a cut to describe the finite duration of excitation. The simple elementary signal (7) can be obtained as an approximation of a pulse-shape function with an instantaneous jump-like decaying phase. Results on simple signals have been presented in [34] for a triangular coupling function with a non-instantaneous decaying phase. Here we complete and develop the analytical study with a particular attention to composite signals.

The results that we will analyze are numerically illustrated in Fig. 1 where simple signals ( $s = 0$ ) and composite signals ( $s \neq 0$ ) are investigated. Numerical simulations are made using a time stepping method where, at each time step, new emission times are found by threshold-crossing detection. The calculated emission times are propagated to neighboring elements and the network state is updated using the coupling function. In Fig. 1(a) the existence of simple signals is studied with the plot of the traveling wave speed  $c$  as a function of the total connectivity strength,  $|w| = \sum_i w_i$ . When  $|w|$  is small, there is no traveling signals and propagation failure is observed. Depending on the connectivity, three branches of solutions can be found, reported as 1-signal, 2-signal and 3-signal (and noted 1S, 2S and 3S), from bottom to top, respectively. Candidate solutions for both simple and composite signals are obtained in Fig. 1(b) in the  $(c^{-1}, s)$  plane as the crossing points of the two level curves (4). Using (7), it is easy to see that the level curves have a graph that is composed of three distinct segments that can be determined analytically as a function of the weights,  $w_i$ . Inspection of the threshold condition, shown in Fig. 1(c), reveals that a candidate solution may violate the causality criterion and, as a consequence, parts of the branches shown in Fig. 1(a) do not define admissible solutions. Traveling wave solutions are shown in Fig. 1(e),(f) where depending on the initial excitation, a simple wave or a composite wave propagates along the transmission line.

**Simple signals.** The analytical description of the speed diagram of simple waves is derived from the threshold condition  $\sum_i w_i e(i/c) = 1$  and it is easy to show that the velocity,  $c$ , as a function of the global connectivity strength,  $|w|$ , is composed of three branches. As  $c$  varied, jumps at the two critical speeds  $c = 3$  and  $c = 2$  indicate the transitions from 3-signal to 2-signal and from 2-signal to 1-signal, respectively. The discontinuity of the speed curve is the result of the instantaneous decrease of the coupling function. The transmission speed associated with the different branches is given by

$$c_p = \sum_{i=1}^p i w_i, \quad (8)$$

where  $p = 1, 2, 3$  for  $p$ -signals. It is interesting to see that the connectivity of the transmission line can be reconstructed from the velocity of propagating signals using recursively the formula,  $w_1 = c_1$ ,  $w_i = (c_i - c_{i-1})/i$ ,  $i = 2, 3$ . Therefore the full network connectivity can be inferred from the observation of three distinct propagat-

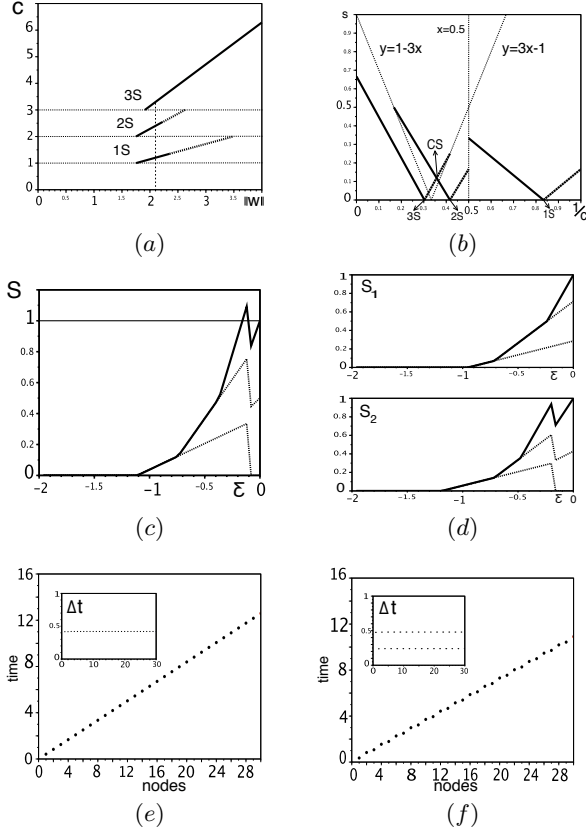


FIG. 1. Traveling signals along the transmission line for a connectivity given by  $w_1 = 4|w|/7$ ,  $w_2 = w_1/2$  and  $w_3 = w_2/2$ . (a) Speed diagram of simple signals where the velocity  $c$  of the signal is plotted as a function of the global connectivity strength  $|w|$ . The graph is made of three distinct branches, noted 3S, 2S and 1S, from top to bottom, respectively. Dotted lines are for solutions that are not admissible (see panel (c)). The vertical dotted line indicates the value  $|w| = 2.1$  that is used in plot (b) for the graphical representation of the two level curves  $f(x, y) = 0$  and  $f(x, -y) = 0$  (see (4)) in the  $(x, y) = (1/c, s)$  plane. Crossing points indicate candidate solutions for traveling signals. Solutions on the  $x$ -axis, i.e. for  $s = 0$ , are associated with simple signals and the corresponding branch of the speed diagram is mentioned by the labels 3S, 2S or 1S. The label CS indicates a candidate solution for a composite signal. Some candidate solutions are non-admissible as shown in (c) for a solution on the 2S branch of the speed diagram (we use here  $|w| = 2.4$ ) for which the causality criterion is violated. In (d) the signal profiles,  $S_1$  and  $S_2$ , of the composite signal are shown for the solution noted CW in panel (b). Raster plots of the traveling signal for (e) a simple signal and (f) a composite signal. The two insets show the associated inter emitting-time interval, noted  $\Delta t = t_{i+i} - t_i$  where  $i$  is the index of the node.

ing signals.

The threshold condition only gives candidate solutions and the causality criterion (5) determines their admissibility. By inspecting the maximum of the wave function

$S(\xi) = \sum_i w_i e(\xi - i/c)$  in the region  $\xi < 0$ , we determine the exact conditions for the admissibility of the different simple signals. The branch associated with the fast transmission, referred to as the 3S branch, defines strictly increasing traveling wave solutions that are therefore always admissible. For the two other branches, some candidate solutions may be non-admissible as it is shown in Fig. 1(a) where the 2-signal branch and the 1-signal branch corresponds to non-admissible signals when  $|w|$  is large, i.e. greater than  $|w| \sim 2.2$  and  $|w| \sim 2.35$ , respectively, for parameters used in the plot. A propagating signal can be found on the  $p^{\text{th}}$  branch of the speed curve if the following conditions hold: for  $p = 2$ ,  $w_1 + w_2 > 2w_3$  and for  $p = 1$ ,  $w_1 > \min(w_2, w_3)$ .

The stability of simple waves is determined from (6) that, after factoring by  $\lambda - 1$ , reduces to a second order polynomial and it is easy to demonstrate that simple signals are always stable.

**Composite signals.** The transmission of a time interval different from the one trivially associated with the wave speed is less well understood and studied. Exploration of candidate solutions for system (4) using the coupling function (7) leads to a viability region, i.e. a region where admissible composite signals may be found, that can be determined explicitly in the  $(1/c, s)$  plane as depicted in Fig. 2. There are two distinct regions that are related to

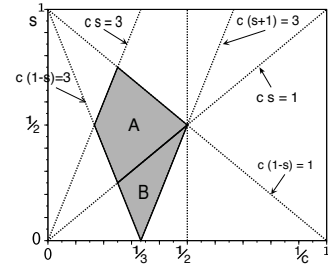


FIG. 2. Locus of existence of composite signals in the  $(c^{-1}, s)$  plane. The grey shaded quadrilateral indicates the region where a composite signal may be found. In region A, where  $cs > 1$ , the firing sequence associated with the propagating signal is non monotonic whereas in region B the wave pattern corresponds to a strictly increasing sequence of firing times. The boundary between the two regions ( $cs = 1$ ) corresponds to the propagation of a pair of synchronous firing times.

different modes of signal propagation. In region labeled A, the propagation is characterised by a non-monotonic sequence of activation times and in region B, the sequence is strictly increasing. When  $w_1 < w_3$ , the signal speed  $c$  and the time interval  $s$  belong to region A (see Fig. 2) and can be determined analytically using the threshold-crossing condition. We find

$$c = \frac{w_1 + w_3}{d_A}, s = \frac{3w_3 - w_1}{d_A}, \quad (9)$$

where the parameter  $d_A$  depends on the connectivity and is given by

$$d_A = 2(w_1 w_2 + w_2 w_3 + 2w_1 w_3).$$

For  $w_1 > w_3$ , candidate solutions are located in region B and are given by

$$c = \frac{3w_3}{d_B}, s = \frac{2w_1 + w_3}{d_B}, \quad (10)$$

where

$$d_B = 2((w_1 + w_2)(w_1 + w_3) + w_1(w_2 + w_3)).$$

Note that when  $w_1 = w_3$ , (9) and (10) coincide. If we note  $c_{cs}$  the velocity of a composite signal, using (8) and (9), (10), we have the following inequalities

$$c_2 \leq c_{cs} \leq c_3,$$

i.e. composite signals travel at a speed intermediate between fast wave speed (velocity of 3-signals) and 2-signal speed.

Using (3), we find that the activity of the nodes described by the waveform  $S_1$  is strictly increasing whereas nodes described by  $S_2$  has a trajectory having a jump down at  $\xi = 1 - 3/c - s$ . Therefore the admissibility condition (5) for composite signals depends only on the wave function  $S_2$  and simply reads as  $S_2(1 - 3/c - s) < 1$  (where the left side limit of the function has to be considered). We obtain the admissibility condition

$$w_1(2/c - 1) + w_2(1/c + s - 1) - w_3 + 1 > 0, \quad (11)$$

where  $(c, s)$  is given by (9) when  $w_1 \leq w_3$  and by (10) when  $w_1 \geq w_3$ . The stability is determined using (6) where the coefficients of the multivariate polynomials are  $a = w_1 \Pi(1/c + s)$ ,  $b = w_2 \Pi(2/c)$ ,  $c = w_3 \Pi(3/c + s)$ , with  $\Pi$  the rectangular function obtained from the derivative of the coupling function  $e$ ,  $\Pi(x) = 1$ , for  $0 < x < 1$  and 0 otherwise. Investigation of the roots (see Appendix B) shows that composite signals are always stable.

The boundary between the two regions, given by  $cs = 1$  and obtained when  $w_1 = w_3$ , is related to the propagation of a synchronous signal where a pair of identical firing times propagates along the transmission line. Synchronous solutions have frequently retained a special attention for their role in conveying and processing information. Precisely synchronized action potentials with millisecond precision can propagate in cortical neural networks [5] and are supposed to play an important role in network remodeling through spike timing-dependent plasticity [9].

**Synchronous waves.** Existence of a synchronous solution is only possible when  $w_1 = w_3$  and we find a propagation velocity  $c = 2(w_1 + w_2)$  that defines a candidate solution when  $w_1 + w_2 > 1$ . The transmitted time-interval is given by  $s = 1/(2(w_1 + w_2))$  and the wave profile is described by the two following functions. The first wave function is given by

$$S_1(\xi) = (w_1 + w_2)\xi + 1,$$

for  $-2/c \leq \xi \leq 0$  and 0 otherwise. The second wave shape is defined by

$$S_2(\xi) = w_1 \xi + \frac{2w_1}{w_1 + w_2},$$

for  $-4/c \leq \xi \leq -2/c$ , and

$$S_2(\xi) = (2w_1 + w_2)\xi + \frac{2w_1}{w_1 + w_2} + 1,$$

for  $-2/c \leq \xi \leq 1 - 4/c$ , and

$$S_2(\xi) = (w_1 + w_2)\xi + 1,$$

for  $1 - 4/c \leq \xi \leq 0$ . The waveform is strictly increasing for the nodes associated with  $S_1$  whereas the function  $S_2$  presents a jump of discontinuity,  $\Delta S_2 = -w_1$ , at  $\xi = 1 - 4/c$ . The admissibility condition (11) reads  $2w_1 + w_2 < 2$ . The locus of existence of synchronous waves in the  $(w_1, w_2)$ -parameter plane is plotted in Fig. 3 and is compared with the regions of existence of simple signals. A large part of the parameter space  $(w_1, w_2) \in$

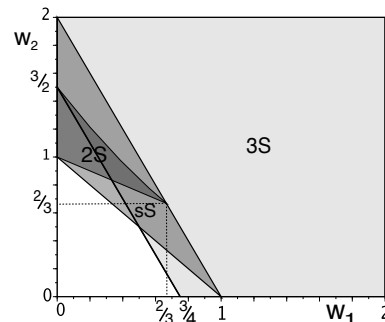


FIG. 3. Regions of existence of a stable signal transmission in the  $(w_1, w_2)$  plane for  $w_1 = w_3$ . A signal can propagate stably along the transmission line for parameters in the grey regions. Different areas are depicted with different grey levels that represent simple signals, labeled 3S and 2S, and composite signals, noted sS for synchronous signal. The region 3S is a half plane delimited by the straight line  $2(w_1 + w_2) = 3$ . The zone labeled ‘sS’ is triangular and the 2S region is triangular in shape.

$\mathcal{R}_+^2$  corresponds to the propagation of simple signals where 3-signals are the dominant patterns. The 1-signal does not exist when  $w_1 = w_3$  (causality criterion is violated) but 2-signals transmission is possible. Propagation failure is observed when both  $w_1$  and  $w_2$  are small. There exist regimes where synchronous waves can travel for parameters where simple signals are also free to travel, i.e. the transmission line presents a bistability between simple and synchronous waves, the initial stimulation determines the propagating pattern. In particular, 2-signals always coexist with synchronous signals. Interestingly there also exists a tiny region where the synchronous

wave can travel in parameter regimes where simple signals fail to propagate. For instance when  $w_1 = w_3 = 0.3$  and  $w_2 = 0.8$ , the propagation of a synchronous wave is observed whereas simple waves do not exist.

As  $w_1$  changed, different regimes can be reached. If we set  $w_2 = 0.8$ , the following sequence of bifurcations, as  $w_1$  increased, is observed. At small  $w_1$  values, signals do not propagate along the network. As  $w_1$  reaches the critical value  $w_1 = 1 - w_2 = 0.2$ , synchronous waves appear. When  $w_1$  reaches the value  $3/4 - w_2/2 = 0.35$ , there is a coexistence between synchronous waves and 3-signals, and subsequently when  $w_1 = 2 - 2w_2 = 0.4$  a tristability regime with the possible propagation of 2-signals.

## V. DISCUSSION

Cellular automata are minimal models that describe the dynamics of excitable media [14, 36] where the propagation results from a cooperative effect generated and transmitted by simple identical and connected components [39]. Despite the strong similarities with the propagating patterns generated by more realistic models, as spiking neural lattice for instance [21], cellular automata do not capture the temporally continuous properties of excitable systems and their sensitivity to the updating scheme made them inadequate for describing natural processes.

In this paper, we formulated a simple phenomenological model of excitable media consisting of a continuous time-integration of incoming signals supplemented with a threshold effect. The resulting model is an information-processing line that allows for stable signal transmission with different velocities, as observed in one-dimensional neuronal cultures [8]. Classical solutions described by a unique waveform are obtained but more complex trajectories composed of multiple profiles also exist. Using a simple activation function the model is solvable and the propagation of composite waves is studied in detail. The stability of traveling signals with several distinct profiles is shown. The exact dependence of the traveling signals on the connectivity of the network is obtained for the propagation of a doublet including the case of synchronous propagation.

We consider a network with third-nearest-neighbor coupling that allows for the temporal repetition of a doublet along the line. The doublet is not generated by the re-excitation of nodes but is an intrinsic property of the network. It would be interesting to study the propagation of larger sequences, i.e. triplet or quadruplet, that can occur in a transmission line with an extended connectivity. Simulations (not shown) reveal that long range interactions give rise to more complex signals and future works are necessary to clarify the link between connectivity footprint and signal propagation. Another further extension of this work will concern the effect of multiple-activation of nodes. We restrict our attention here to the so called one-spike framework where nodes

can emit only one time and interactions between several activation-times would create a richer variety of phenomena. Fixed profiles that change cyclically are studied here but irregular patterns that evolve continually may also exist. The case of quasi periodic solutions, not studied here, could be considered to broaden possible signal transmissions in the network.

## APPENDIX A

**Simple waves for  $w_1 = w_3$ .** For a transmission line such that  $n = 3$  and  $w_1 = w_3$ , the existence of  $p$ -waves is given by the following conditions. The fast wave speed ( $p = 3$ ) is given by  $c = 4w_1 + 2w_2$  and the condition  $c \geq 3$  reads  $w_2 \geq 3/2 - 2w_1$ . For  $p = 2$ , we have  $c = w_1 + w_2$  and conditions  $2 \leq c \leq 3$  gives  $1 - w_1/2 \leq w_2 \leq 3/2 - w_1/2$ . For the slow wave, i.e.  $p = 1$ , the wave speed is given by  $c = w_1$  and we obtain the condition  $1 \leq w_1 \leq 2$ .

The candidate solution defines an effective solution if the admissibility condition  $S(\xi) < 1$ , for  $\xi < 0$ , is fulfilled. As previously mentioned, fast waves (3-signals) are always admissible solutions. Using  $\max_{\xi < 0} S(\xi) < 1$ , we find the following admissibility condition for 2-waves:

$$2w_2^2 + 2w_1^2 + 5w_1w_2 - 3w_2 - 3w_1 < 0.$$

One can show that the condition of existence for 2-signals  $w_2 \leq 3/2 - w_1/2$  is fulfilled when the admissibility condition holds. For 1-wave we find the admissibility condition  $w_1 < 1$  that is in contradiction with the existence criterion and therefore the branch of 1-wave solutions is not admissible.

## APPENDIX B

**Stability analysis of composite signals.** We distinguish between the two regions of existence of composite signals (see Fig.2)

Case A:  $w_1 \leq w_3$ . From (6), we study the roots  $(\lambda_1, \lambda_2)$  of the multivariate polynomials

$$\begin{aligned} (w_2 + w_3)xy^2 - w_2y - w_3 &= 0, \\ (w_1 + w_2)x^2y - w_1xy - w_2x &= 0. \end{aligned}$$

The trivial solutions  $\lambda_1 = \lambda_2 = 1$  and  $\lambda_1 = 0$  are handled easily and we end up with

$$\lambda_1\lambda_2 = \frac{w_2^2 - w_1w_3}{(w_1 + w_2)(w_2 + w_3)}$$

and we find that  $|\lambda_1\lambda_2| < 1$  is always satisfied showing the stability of composite signals.

Case B:  $w_1 \geq w_3$ . System (6) gives

$$\begin{aligned} xy^2 - w_1xy - w_2y - w_1 + w_2 &= 0, \\ (w_1 + w_2)x^2y - w_1xy - w_2x &= 0, \end{aligned}$$

that, after dealing with the trivial cases, leads to:

$$\lambda_1 \lambda_2 = \frac{w_2^2 - w_1 w_3}{(w_1 + w_2)(w_1 + w_2 + w_3)}.$$

It follows that  $|\lambda_1 \lambda_2| < 1$  and the stability of the associated traveling signal.

- 
- [1] M. Abeles, H. Bergman, E. Margalit, and E. Vaadia, *J. Neurophysiol.* 70, 1629 (1993).
- [2] A. Aertsen, M. Diesmann, and M. O. Gewaltig, *J. Physiol. Paris* 90, 243 (1996).
- [3] A. Arenas, A. Díaz-Guilera, and C.J. Pérez-Vicente, *Phys. Rev. Lett.* 96, 114102 (2006).
- [4] P. C. Bressloff, *Phys. Rev. Lett.* 82, 2979 (1999).
- [5] M. Diesmann, M. O. Gewaltig, and A. Aertsen, *Nature* 402, 529 (1999).
- [6] R. Eckhorn, *IEEE trans. Neural Netw.* 10, 464 (2003).
- [7] G. B. Ermentrout, *J. Comput. Neurosci.* 5, 191 (1998).
- [8] O. Feinerman, M. Segal and E. Moses, *J. Neurophysiol.* 94, 3406 (2005).
- [9] W. Gerstner, R. Kempter, and J.L. van Hemmen, and H. Wagner, *Nature* 386, 76 (1996).
- [10] W. Gerstner and W.M. Kistler, *Spiking neuron models* (Cambridge University Press, 2002).
- [11] J. Gorecki, J.N. Gorecka, and Y. Igarashi, *Natural Computing* 8, 473 (2009).
- [12] D. Golomb and E. Ermentrout, *Proc. Natl. Acad. Sci.* 96, 13480 (1999).
- [13] D. Golomb, X.J. Wang, and J. Rinzel, *J. Neurophysiol.* 75, 750 (1996).
- [14] J. M. Greenberg and S. P. Hastings, *SIAM J. Appl. Math.* 54, 515 (1978).
- [15] P. Grindrod, *Patterns and waves: the theory and applications of reaction-diffusion equations* (Oxford University Press 2nd edition, 1996).
- [16] A. Hoffman and J. D. Wright, *Phys. D: Nonlinear Phenom.* 358, 33 (2017).
- [17] A.V. Holden, J.V. Tucker, and B.C. Thompson, *Phys. D: Nonlinear Phenom.* 49, 240 (1991).
- [18] H. J. Hupkes, L. Morelli, and P. Stehlík, *SIAM J. Appl. Dyn. Syst.* 18, 973 (2019).
- [19] H. J. Hupkes, L. Morelli, P. Stehlík, and V. Svígler, *Appl. Math. Comput.* 361, 430 (2019).
- [20] V. K. Jirsa, *Neuroinformatics* 3, 183 (2004).
- [21] V. B. Kazantsev, V. I. Nekorkin, S. Binczak, and J. M. Bilbault, *Phys. Rev. E* 68, 017201 (2003).
- [22] H. Markram, W. Gerstner, and P. J. Sjöström, *Front. Synaptic Neurosci.* 4, 2 (2012).
- [23] J. D. Murray, *Mathematical Biology*, (Springer, Berlin 1990).
- [24] V. Pérez-Munuzuri, V. Pérez-Villar, and L.O. Chua, *Int. J. Bifur. Chaos* 2, 403 (1992).
- [25] A. Pérez-Munuzuri, V. Pérez-Munuzuri, V. Pérez-Villar, and L.O. Chua, *IEEE Trans. Circuits Syst.* 40, 872 (1993).
- [26] B. Prasse and P.V. Miegheem, *Proc. Natl. Acad. Sci.* 119 (2022).
- [27] J. Rinzel, D. Terman, X.-J. Wang, and B. Ermentrout, *Science* 279, 1351 (1998).
- [28] J. Teramae and T. Fukai, *Biol. Cybern.* 99, 105 (2008).
- [29] S. Thorpe, A. Delorme, and R. Van Rullen, *Neural Netw.* 14, 715 (2001).
- [30] M. Timme, *Phys. Rev. Lett.* 98, 224101 (2007).
- [31] M. Timme and J. Nagler, *Nat. Phys.* 15, 308 (2019).
- [32] M. Toda, *J. Phys. Soc. Japan.* 23, 501 (1967).
- [33] A. Tonnelier, *SIAM J. Appl. Dyn. Syst.* 9, 1090 (2010).
- [34] A. Tonnelier, *SIAM J. Appl. Dyn. Syst.* 18 (2019).
- [35] R. Erazo-Toscano and R. Osan, *Phys. Rev. E* 107 (2023).
- [36] J. R. Weimar, J. J. Tyson, and L. T. Watson, *Phys. D: Nonlinear Phenom.* 55, 309 (1992).
- [37] A. T. Winfree, *Chaos* 3, 303 (1991).
- [38] H.R. Wilson, R. Blake, and S.H. Lee, *Nature* 412, 907 (2001).
- [39] S. Wolfram, *Nature* 311, 419 (1984).